Phase composition, microstructure and microhardness of electroless nickel composite coating co-deposited with SiC on cast aluminium LM24 alloy substrate

Phase composition, microstructure and microhardness of electroless nickel composite coating co-deposited with SiC on cast aluminium LM24 alloy substrate.

M. Franco[1], W. Sha[1,*], S. Malinov[2], R. Rajendran[3]

[1]School of Planning, Architecture and Civil Engineering, Queen's University Belfast, Belfast BT7 1NN, UK

[2]School of Mechanical and Aerospace Engineering, Queen's University Belfast, Belfast BT7 1NN, UK

[3]School of Mechanical and Building Sciences, B. S. Abdur Rahman University, Chennai 600048, India

Abstract: Electroless Ni-P (EN) and composite Ni-P-SiC (ENC) coatings were developed on cast aluminium alloy substrate, LM24. The coating phase composition, microstructure and microhardness were investigated using X-ray diffraction (XRD), scanning electron microscopy (SEM) and microhardness tester, respectively, on as-plated and heat-treated specimens. The original microstructure of the Ni-P matrix is not affected by the inclusion of the hard particles SiC. No formation of Ni-Si phase was observed up to 500°C of heat treatment. The microhardness is increased on incorporation of SiC in Ni-P matrix. The hardening mechanism is the formation of intermetallic phase Ni_3P on annealing at elevated temperature.

Keywords: Aluminium; Electroless Ni-P-SiC; Phase transitions; Scanning electron microscopy; Microhardness

* Corresponding author. Tel.: +44 28 90974017; fax: +44 28 90974278.
E-mail address: w.sha@qub.ac.uk (W. Sha).

1. Introduction

The recognition of electroless nickel plating (EN) has been increasing since its inception in the mid twentieth century [1] owing to the outstanding properties such as excellent uniformity on complex geometry, high hardness and good corrosion resistance which are the concerned properties for engineering applications [2-4]. The quest for improved coating properties has led to the development of relatively new electroless coating known as "electroless nickel composite coating" (ENC) by incorporating hard or soft particles in the Ni-P matrix. The impregnation of hard particles such as silicon carbide (SiC), alumina (Al_2O_3) and boron carbide (B_4C) escalates hardness and wear properties [5-8]. On the other hand, soft particles such as MoS_2, PTFE, graphite etc. make the coating preferable for lubricating application.

Among the composite coatings containing hard particles, the coating obtained by the co-deposition of SiC particles with Ni-P matrix has proved to be the most cost-effective and best performing combination in application areas where hardness and abrasive is the main requirement [9]. Several researchers [10-13] investigated the hardness property of SiC incorporated electroless Ni-P coating and found it improved. On increasing the heat treatment temperature upto 400°C, same trend of increase in the hardness is found for both EN and ENC samples. The hardening mechanism is the same for both EN and ENC coatings which is due to the formation of intermetallic Ni_3P phase. The SiC particles remain thermally stable and well supported by hardened metal matrix upon heat treatment upto 400°C [9, 10, 12-14].

For composite Ni-P-SiC (ENC), in general, many investigators observed the non-interference of the SiC particles with the original structure of nickel matrix. In other words, the particles are simply enveloped in the metal matrix by impingement and settling on the surface of the specimen during the course of coating development without affecting the original microstructure of metal matrix [5, 6, 11, 15]. On annealing at elevated temperature, crystallization occurs with the formation of Ni_3P giving rise to many sharp X-ray diffraction

peaks. The SiC peaks remain identical over the heating process which confirms the stability of Si-C bond. However, the bonding reaction occurs at 650°C [13] resulting in the formation Ni_3Si. Chen et al. [14] observed the decomposition of SiC above 450°C and reaction occurs with nickel to form Ni_5Si_2 and β_1-Ni_3Si. Broszeit [16] found the formation of Ni_3Si at 580°C in composite ENC samples. Though there were several studies of heat treatment done on the composite coating, there is lack of consistency in the findings of the thermal stability range of the SiC in the metal matrix affecting the coating properties.

In general, hardness is considered as an important material characteristic because the wide practical applications rely heavily on the hardness. The wear and tear properties of the material are related to the hardness of the material. Therefore, the study on the hardness might be able to identify some important aspects of the composite coating quality onto cast Al-Si alloy (LM24) viable to be used as cylinder liner application in automobile engine domain which is the primary concern of the current work.

Al-Si alloys are increasingly used in automotive engine blocks due to their lighter weight and better heat conductivity than cast iron. Cast Al-Si having excellent castability are suitable for many complex automotive designs such as pistons, engine blocks, cylinder liners, cylinder heads and wheels. However, the Al-Si alloy suffers from insufficient hardness and wear resistance [4].

The main aim of the work is to study the coating properties specifically phase compositions, microstructure, surface roughness and microhardness of the electroless nickel composite coating co-deposited with hard particles SiC onto the lightweight aluminium LM24 alloy. In composite coating preparation, liquid flow becomes very important as it will determine the degree of deposition of the second phase particles. Many papers deal with unidirectional codeposition using magnetic stirrer but the present study makes use of an additional sample rotator at low speed against the direction of the liquid flow produced by magnetic stirrer.

2. Experimental details

2.1. Preparation of electroless nickel composite coatings

Aluminium alloy (LM24) samples of dimension 50 mm × 50 mm × 2 mm were prepared by using electrical discharge machining (EDM). The samples were pre-treated for cleaning, prior to plating, using acetone degreasing, followed by alkaline cleaning and then by acid neutralising. Zincating was done to improve the adhesion of the coating. Each step is followed by deionised water rinsing. The details of the pre-treatment process are given in table I. Plating was performed using a medium phosphorus commercial electroless solution (NiKlad ELV 808MX, MacDermid). The plating conditions are shown in table II. However, MacDermid which is the plating solution supplier would not disclose its composition (formulation). Electroless nickel composite coating was prepared by introducing silicon carbide (SiC, particle size range 1-7 μm) in the plating solution. Concentrations of SiC in the range of 2-18 g/l were used to study the effect on the coating properties. For comparison purpose between particles free and with particles, 2.2 g/l of SiC was taken arbitrarily, based on the concentration range used in literature [8, 17]. Prior to introduction into bulk plating solution, the hard particles (SiC) was stirred in a small part (about 200 ml) of plating solution by using magnetic stirrer to facilitate homogenous suspension of the hard particles and then poured into the bulk plating solution. The stirring speed was kept constant throughout the process for all the samples. The flow of the plating solution was circular along with the particles in suspension and the sample was rotated at low speed against the direction of the liquid flow. The sample rotator speed and the magnetic stirrer speed were chosen after several trials for uniformity and proper suspension of the second phase particles with minimum settling at the bottom. For increasing and decreasing of pH, dil. ammonium hydroxide (~50% vol.) and 10% vol. H_2SO_4 were used respectively. The plated samples were cut into smaller pieces for X-ray diffraction (XRD), scanning electron microscopy (SEM), surface roughness and microhardness measurements.

Electroless nickel samples (EN and ENC) were heat treated isothermally in a furnace at atmospheric pressure. The samples were placed in a pre-heated condition and held for 1 h at various temperatures, 200°C, 300°C, 400°C and 500°C and subsequently cooled down to ambient condition.

2.2. Surface and cross-section analysis of the coatings

XRD analysis on the EN and ENC samples was carried out at room temperature using PANalytical X-ray diffractometer applying CuK_{α} radiation of wavelength 1.541874 Å. The step size of scans was 0.02°. The integrated software X-Pert high score was used to analyse the phase compositions and the peaks refinement was done using Profile Fitting to obtain quantitative measurable values for peak information such as Full Width Half Maximum (FWHM) and corresponding peak locations (diffraction angle).

FE-SEM (QUANTA FEG250) equipped with OXFORD X-Act as chemical composition analyser was used to study the surface morphology and microscopic changes of the coating during heat treatment. Energy dispersive X-ray (EDX) run by Aztec version 2.0 software was used for chemical composition analysis.

Surface roughness was measured using Rugosurf 10G roughness tester, cut-off length of 0.8 mm, following the standard ISO 4287:1997. The calibration was done on reference sample at room temperature, prior to the measurements on EN and ENC samples, keeping all the samples and instrument set on a vibration free desk. The average roughness (Ra) is obtained from three readings measured at different locations on the samples.

Microhardness of the samples was measured using Mitutoyo series HM-124 microindentation hardness tester (with an integrated optical microscope of magnification 100× and an eye-piece micrometer measuring system). The measurements were done on polished cross section of EN and ENC samples both in as-deposited and heat-treated conditions. Knoop indenter was used with a load of 50 gf for EN and ENC samples for comparison purpose. Load of 100 gf was

applied for the higher concentrations of SiC in order to have a clear impression mark for easy hardness measurements. The cross section samples were prepared metallographically which involves hot mounting using carbon based resin, grinding and polishing. The reported results are the average of six indentations measured at different locations for each sample. The error bar is based on the standard deviation (±) corresponding to the average hardness for each sample.

3. Results and discussion

3.1. Phase structure

Fig. 1 shows the X-ray diffraction (XRD) patterns for all the electroless nickel samples (without zincating, with zincating and composite coatings). For as-deposited samples, the presence of broad and single peak at the 2θ position 40-50° shows the typical amorphous structure of electroless nickel coating. For phosphorus content around 8.8 wt. % upto temperature ~90°C which is the deposition temperature, the equilibrium phase diagram of Ni-P alloys [18] suggests the equilibrium phases as Ni and Ni_3P. At this temperature (as-deposited condition), phosphorus is virtually insoluble in the nickel lattice, i.e., the formation of equilibrium solid solution of phosphorus in nickel is thermodynamically unstable [9, 19, 20]. This observation is substantiated by the metastable amorphous phase which has the tendency to crystallisation when subjected to thermal treatment at elevated temperatures.

The diffraction patterns for EN samples, both without zincating and with zincating, in as-deposited conditions are similar. The XRD profile for ENC samples is identical to that of EN samples except for the peak corresponding to silicon carbide (SiC) with plane {111} observed at 2θ=35.7° (major peak) which is consistent with other reported work [9, 10, 14].

On heat treatment at 200°C for all the three samples, the broad peak has sharpened slightly. The SiC peak remains the same for composite sample indicating that no side reaction occurs between the metal matrix and the particles at this temperature. The 300°C XRD profiles

exhibit a mixture of amorphous and crystalline phases in which the low temperature single amorphous peak now splits into two (one with higher intensity and the other is tending to evolve at about 2θ=51°) due to reflection predominantly from Ni planes {111} and {200}. On higher temperature annealing at 400°C, several peaks have emerged from the reflection of planes of intermetallic phase, nickel phosphide (Ni_3P) and f.c.c. nickel. As reported by Hentschel et al. [19] and Farber et al. [20], on increasing temperature, a segregation process of phosphorus in the grain boundaries and triple junctions of NiP grains occurs. Subsequently, precipitation of Ni_3P occurs when P-rich zones exceed a certain phosphorus limit. It is diffusion control process in which nickel atom is assumed to have migrated through P-rich zones and reacted with phosphorus to form Ni_3P [9]. The formation of intermetallic phase Ni_3P results in volumetric shrinkage with grain size increasing. Hence it results in the formation of sharp crystalline peaks in the X-ray profile. The evolution of much sharper peaks is the indication of increase in grain size upon heat treatment. No additional formation of Ni_xP_y phases is seen on annealing up to 400°C. Apparently, the metastable intermediate phases might have decomposed during isothermal holding for 1 h at this temperature, which is also supported by the theory of phase transformation [3]. The metastable phases like Ni_2P and $Ni_{12}P_5$ might have transformed to a more stable phase Ni_3P during the course of heating for 1 h.

The high temperature XRD profiles for electroless nickel composite (ENC) samples is much similar to those of EN samples. At 400°C heat treatment, the peak corresponding to SiC still exists with neither shifting of 2θ position nor formation of additional peaks consisting of silicon, indicating the thermal stability of Si-C bond resulting in no side bond formation with the metal matrix (NiP) or with other elements. The observation is a confirmation of the fact that there is no molecular bonding mechanism between the particles and metal matrix for the formation of composite coating but an impingement and settling of particles on the surface and subsequent envelopment of these particles by the matrix material [5, 15]. On further

annealing up to 500°C, there is no evidence of the formation of Ni_xSi_y implying that the stability of SiC still persists. However, the sharpness of the SiC peak starts declining. In other word, the peak broadens slightly which is evident from the peak broadening values (Table III).

Table III shows the FWHM of the selected planes of Ni {111}, Ni {200}, Ni_3P {231} and SiC {111} to show the quantitative changes in the peak width as a function of heat treatment at various temperatures. The FWHM values for all Ni and Ni_3P peaks become smaller on increasing the annealing temperature, indicating the sharpening of the peaks which clearly agrees the evolution of crystallization at elevated temperature. The FWHM values for the SiC peak in the ENC sample heat treated at 300-500°C exhibit increase which might be attributed to the onset of Si-C bond weakening as the complexity of SiC occurs on elevated temperature which is considered as one of the drawbacks for composite coating [14]. As mentioned earlier, the absence of the formation of additional phases Ni_xSi_y concludes firm evidence that up to 500°C, SiC exists in its original structure. Hence, the hard particles SiC remains enveloped in the Ni-P matrix as before up to this temperature of heat treatment.

3.2. Surface morphology and chemical composition

The surface morphology of the electroless coatings is shown in figs. 2 and 3. The coating thickness is 25-30 μm. The cauliflower morphology of the samples is consistent with the literature. For electroless composite samples the hard particles are distributed uniformly, entrapped in the nickel-phosphorus matrix. The composite coating shows some micro pores which might be the marks for particles' temporary existence before falling off due to improper envelopment in metal matrix owing to slow deposition during plating process. Li et al. [13], Yang et al. [17] and Huang et al. [21] observed the existence of pores as well in the electroless nickel composite coating. The samples heat treated at 400°C exhibit more pores as compared to as-deposited condition for both the EN and ENC samples which might be

attributed to the void created by the release of trapped hydrogen gas during the course of annealing. It is worth mentioning that during the process of plating, enormous amount of hydrogen gas is liberated at the vicinity of the work piece (sample), so metal deposition is accompanied by hydrogen gas entrapment [2]. Thus, on heat treatment the entrapped hydrogen gas is liberated creating voids in the coating which is a common microscopic feature of electroless nickel coatings [2].

The heat-treated samples (cross section) for both EN and ENC samples show some micro cracks and flakes on the edge of the coating which is at the surface portion (figs. 4b and 4d). This observation indicates the typical brittleness of the electroless nickel coating [2] but may also be due to oxidation during heating in air. The flakes observed only at the surface portion but not at the interface between the coating and the substrate is a rough indication about the good adhesion of the coating onto the substrate. The bonding between the coating and the substrate appears to be more firm and compact upon heat treatment which is supported by the absence of narrow groove along the substrate's contour at the interface as compared to as-deposited condition (figs. 4a and 4c) for both the EN and ENC samples. The micrographs of the cross section samples show the uniformity of the coating that follows the contours of the substrate.

The energy dispersive X-ray (EDX) spectrometry was used to measure the weight percentage of phosphorus in the electroless nickel coating. It was found that the phosphorus content is 8.8 wt. % (Table IV) which agrees with the technical data from the plating solution supplier. The type of electroless nickel coating is medium phosphorus electroless nickel plating of nominal content (7-9.5 wt. % of P). For composite ENC sample, three EDX spectra (fig. 5) were taken to analyse the hard particles (SiC) weight percentage in the coating. The element carbon is not detected in the spectra so the weight percentage of carbon is calculated from the stoichiometric ratio of the chemical composition of SiC considering 1:1 ratio as

$$wt.\ of\ carbon = \frac{atomic\ wt.of\ carbon \times wt.of\ silicon\ in\ spectrum}{atomic\ wt.of\ silicon}$$

Thus the weight of silicon carbide is the sum of the calculated weight of carbon and weight of silicon from the spectrum. The new weight percentage of the elements normalised to hundred is obtained dividing the weight of the element from spectrum by the new total weight, multiplied by hundred. The average of the weight percentage of each element (Table IV) is derived from the three spectra and ± (standard deviation) is used to indicate the errors. The weight percentage of SiC in the coating is approximately consistent with the results of Cheng et al. [6] considering the similar SiC concentration in the plating solution.

3.3. Surface roughness

The roughness of the substrate is reduced on coating with electroless nickel. The particles free EN coating has least roughness (Table V). As expected, the hard particles co-deposition ENC samples have increased roughness which is in agreement with Apachitei et al. [9]. Due to the entrapment of the particles, the NiP matrix grows around the particles during autocatalytic process. When the deposition is stopped at a certain time, many protruding particles are left uncovered. Thus these irregular protruded particles roughen the surface.

3.4. Hardness

Microhardness for EN (particle free) coating in as deposited condition for both with zincating and without zincating is more or less the same. As it is clearly visible in the bar chart shown in fig. 6, there is no large variation in hardness values for without zincating and with zincating samples.

On heat treatment at 200°C there is slight improvement of hardness for both EN samples. This may be due to the onset of hardening effect, attributed by the tendency of crystallization to a stable phase. A drastic shift to a much higher hardness is found when subjected to 400°C. The temperature range, 300-400 °C, gives the peak hardening effect as reported in several papers

[3-6, 8-12]. One hardening effect is due to the crystallization of intermetallic compound Ni_3P accompanied by high internal stress owing to volumetric shrinkage. Comparing the hardness of heat-treated without zincating and with zincating samples at 400°C, the former exhibits a little higher hardness than the latter, however, there is not much difference. Hence zincating does not contribute significantly to the hardness of the coating.

Electroless nickel composite (ENC) coating has improved hardness in as-deposited condition as compared to particle free electroless nickel (EN) coatings. The maximum hardness reading of 594 $HK_{0.05}$ and a minimum of 420 $HK_{0.05}$ were obtained in as-deposited samples. The variation may be due to the distribution of SiC particles in the nickel matrix. The hardness is further increased on heat treatment at 200°C. The mechanism of the hardening may be similar to that of heat-treated EN samples. On increasing of annealing temperature to 400°C, significant improvement of hardness is seen in the ENC samples. At this elevated temperature, the variation of hardness calculated from different indent marks is smaller compared to those at low temperature samples because the hard particles silicon carbide are well supported by the hardened and stable nickel matrix [12]. Overall, microhardness of the electroless nickel composite (ENC) coating is found to be superior to particle free electroless nickel (EN) coating in both as-deposited and heat-treated conditions.

3.5. Effect of SiC concentration in the plating solution on the coating properties

The optical images shown in fig. 7 are the cross section of composite coatings prepared with the variation of SiC concentration in the plating solution. In all the images, the particles are distributed uniformly in the metal matrix at same distances to the solution sides. However, the incorporation is less at the interface of the coating with the substrate. It is also clearly seen that the second phase particles are deposited scantily when the concentration is low in the plating solution. 2 g/l of SiC gave the least incorporation in the metal matrix (fig. 7a). On increasing the concentrations, the particles are increasingly co-deposited with the metal

matrix. Maximum codeposition of the particles is seen in fig. 7e. The significant change of incorporation level of the hard particles is observed when comparing between fig. 7a and fig. 7e. Hence, SiC concentration in the plating solution plays a role in the composition of the composite coating, Ni-P-SiC.

The microhardness of the ENC coatings as a function of SiC concentration is given in fig. 8. A linear increase in hardness value is observed on increasing the concentration of SiC up to 6 g/l. However, the variation of microhardness is not observed significantly after 6 g/l of SiC because the error bars of all the microhardness values corresponding to the concentrations of 6 g/l and above are within a same value. One reason for no significant change in the microhardness values beyond a particular concentration might be the limited capability of the softer metal matrix to support the particles. If the hardness of the metal matrix is closer to that of the second phase particles, then there might be obvious change in the hardness values with the variation in the concentration of the particles. Hence, it can be concluded that increase in concentration of SiC in the plating solution increases the incorporation level in the coating and thereby increases the microhardness up to a certain concentration beyond which there is no distinct change.

The thickness of the ENC coatings with the change in concentrations of SiC is shown in fig. 9. The thickness appears to be slightly decreasing on increasing the concentration of the second phase particles, SiC, to beyond 6 g/l. This may be attributed to the fact that the deposition of metal matrix is relatively hindered owing to the presence of higher concentration of the particles at the vicinity of the substrate (work piece) during the plating process. However, the change in the thickness build-up is not very large.

3.6. Discussion on differences between electrodeposited and electroless composite coating

Particle charging is more relevant to electroplating, where voltage is applied and there is external current (external to the substrate) in plating solution. Different models and

mechanisms were proposed by many researchers which are primarily related to reduction of metal ions and co-deposition of the second phase particles driven by current densities from various methods such as direct current, pulsed direct current, pulsed reverse current, potentiostatic and pulse potentiostatic. The most common mechanism for the co-deposition of the second phase particles in the metal matrix for electrodeposition involves the charge distribution over the ions in the solution, convection movement towards the cathode, and formation of electrical double layer at the vicinity of the cathode which is followed by adsorption [22]. The electroless composite formation is simply an impingement of the particles along with the metal atoms during reduction process in the presence of reducing agent [5].

In the formation of composite coating by electrodeposition the starting phase (as deposited condition) is perfectly crystalline, so the grain size and shape of the parent phase are more important. On the other hand, the electroless composite coating has amorphous as starting phase, as the Ni-P coatings in the present study are, so the grain size and shape of the parent phase has little relevance. Essentially, the amorphous microstructure is simple, compared to crystalline materials, and the formation of new crystalline phase(s) in it is so much more determined by the big thermodynamic driving force than by the detailed microstructure of the amorphous parent phase, if it has much or any.

4. Conclusion remarks

The following conclusions can be drawn from the findings of the current work

- Electroless nickel plating both particles free (EN) and composite (ENC) co-deposited with hard particles silicon carbide, SiC, were developed on cast aluminium alloy substrate, LM24.
- X-ray diffraction (XRD) analysis on the coatings indicates the formation of intermetallic phase Ni_3P on heat treatment at and above 400°C which is responsible

for hardening of the coatings. There is no evidence for evolution of Ni_xSi_y phase up to 500°C of annealing held for 1 h.

- The original morphology of the Ni-P matrix is preserved after the incorporation of abrasive particles SiC for the composite coating. Some micro pores are seen on the surface of the heat-treated specimens.
- Surface roughness is reduced after coating with EN and ENC. As expected, ENC samples exhibit a little higher surface roughness than EN samples.
- Microhardness is found to be improved on heat treatment for all the EN and ENC samples owing to the crystallisation (formation of intermetallic Ni_3P and Ni) accompanied by volumetric shrinkage and grain growth. Overall, the microhardness of the composite (ENC) coating is found to be superior than particles free (EN) coating in both as-deposited and heat-treated conditions.
- The microhardness increases on increasing the concentration of SiC up to a certain concentration and beyond that there is no large variation.

Acknowledgement

The technical supports from Dr. Mark Russell in getting the XRD and SEM results and Dr. Neil Ogle for isothermal processing work are gratefully appreciated. The authors extend their sincere thanks to Jim Knox and his team of CNC Laboratory, Queen's University Belfast.

References

[1] A. Brenner, G.E. Riddell, J. Res. Natl. Bur. Stand., 37 (1946) 31-34.

[2] D. Baudrand, Electroless nickel plating, ASM Handbook (Vol. 5): Surface Engineering, ASM International, Materials Park, OH, 1994, pp. 290-310.

[3] K.G. Keong, W. Sha, S. Malinov, Surf. Coat. Technol., 168 (2003) 263-274.

[4] R. Rajendran, W. Sha, R. Elansezhian, Surf. Coat. Technol., 205 (2010) 766-772.

[5] J. Balaraju, T. Sankara Narayanan, S. Seshadri, J. Appl. Electrochem., 33 (2003) 807-816.

[6] Yanhai Cheng, Shiju Zhang, Yuxing Peng, Fangfang Xing, Jie Li, Zhencai Zhu, Adv. Mat. Res., 457-458 (2012) 146-149.

[7] J.N. Balaraju, Kalavati, K.S. Rajam, Surf. Coat. Technol., 200 (2006) 3933-3941.

[8] Shusheng Zhang, Kejiang Han, Lin Cheng, Surf. Coat. Technol., 202 (2008) 2807-2812.

[9] I. Apachitei, F.D. Tichelaar, J. Duszczyk, L. Katgerman, Surf. Coat. Technol., 149 (2002) 263-278.

[10] Gao Jiaqiang, Liu Lei, Wu Yating, Shen Bin, Hu Wenbin, Surf. Coat. Technol., 200 (2006) 5836-5842.

[11] Faryad Bigdeli, Saeed Reza Allahkaram, Mater. Design, 30 (2009) 4450-4453.

[12] Xinmin Huang, Zonggang Deng, Plat. Surf. Finish., 80 (1993) 62-65.

[13] Yongjun Li, Plat. Surf. Finish., 84 (1997) 77-81.

[14] C.K. Chen, H.M. Feng, H.C. Lin, M.H. Hon, Thin Solid Films, 416 (2002) 31-37.

[15] A. Grosjean, M. Rezrazi, P. Bercot, M. Tachez, Surf. Coat. Technol., 96 (1998) 14-17.

[16] E. Broszeit, Thin Solid Films, 95 (1982) 133-142.

[17] Gui-rong Yang, Wen-ming Song, Xian-ming Sun, Ying Ma, Yuan Hao, Adv. Mat. Res., 291-294 (2011) 215-218.

[18] Ni (Nickel) Binary Alloy Phase Diagrams, ASM Handbook (Vol. 3): Alloy Phase Diagrams, ASM International, Materials Park, OH, 1992, pp. 2.312–2.322.

[19] Th. Hentschel, D. Isheim, R Kirchheim, F. Müller, H. Kreye, Acta Mater., 48 (2000) 933-941.

[20] B. Färber, E. Cadel, A. Menand, G. Schmitz, R. Kirchheim, Acta Mater., 48 (2000) 789-796.

[21] Y.S. Huang, X.T. Zeng, X.F Hu, F.M. Liu, Electrochim. Acta, 49 (2004) 4313-4319.

[22] C.T.J. Low, R.G.A. Wills, F.C. Walsh, Surf. Coat. Technol., 201 (2006) 371-383.

Table I. Pre-treatment processes of aluminium substrate prior to plating

Process	Chemicals	Concentration	Temperature (°C)	Time (min)	Degree of Agitation
Degreasing	C_6H_6O		Room	3-5	None
Alkaline cleaning	Na_3PO_4	5.75 g/l			
	Na_2O_3Si	5.75 g/l	60-65	3-5	Mild
	Na_2CO_3	1.5 g/l			
Acid neutralising	HNO_3	13 % vol.	Room	3-5	Mild
Zincating	ZnO	100 g/l	Room	0.5-1	Mild
	NaOH	525 g/l			

Table II. Plating process conditions

Processing parameter	Values
pH	4.8-4.9
Temperature	88±2°C
Time	80 min
Silicon carbide (SiC) ccncentration	2-18 g/l
Agitation	Magnetic stirrer along with sample rotator

Table III. FWHM values of selected peaks for EN and ENC samples

Samples	Peaks	FWHM				
		As-deposited	200°C	300°C	400°C	500°C
EN	Ni{111}	-	-	-	0.38	0.22
	Ni{200}	-	-	-	0.46	0.32
	Ni_3P{231}	-	-	-	0.27	0.26
ENC	SiC{111}	0.10	0.11	0.19	0.25	0.20
	Ni{111}	-	-	-	0.49	0.21
	Ni{200}	-	-	-	0.65	0.31
	Ni_3P{231}	-	-	-	0.34	0.25

Table IV. EDX data of elemental weight percentage for the EN and ENC samples

Samples	Element	wt. %
EN	Ni	91.2 ± 0.5
	P	8.8 ± 0.5
ENC	Ni	76.9 ± 2.3
	P	6.4 ± 0.4
	SiC	16.6 ± 2.7

Table V. Roughness (Ra) values for substrate and coatings

Samples	Roughness, Ra (μm)
Bare cast Aluminium substrate	5.07 ± 0.18
EN coated	2.88 ± 0.05
ENC coated	3.13 ± 0.39

List of figure captions

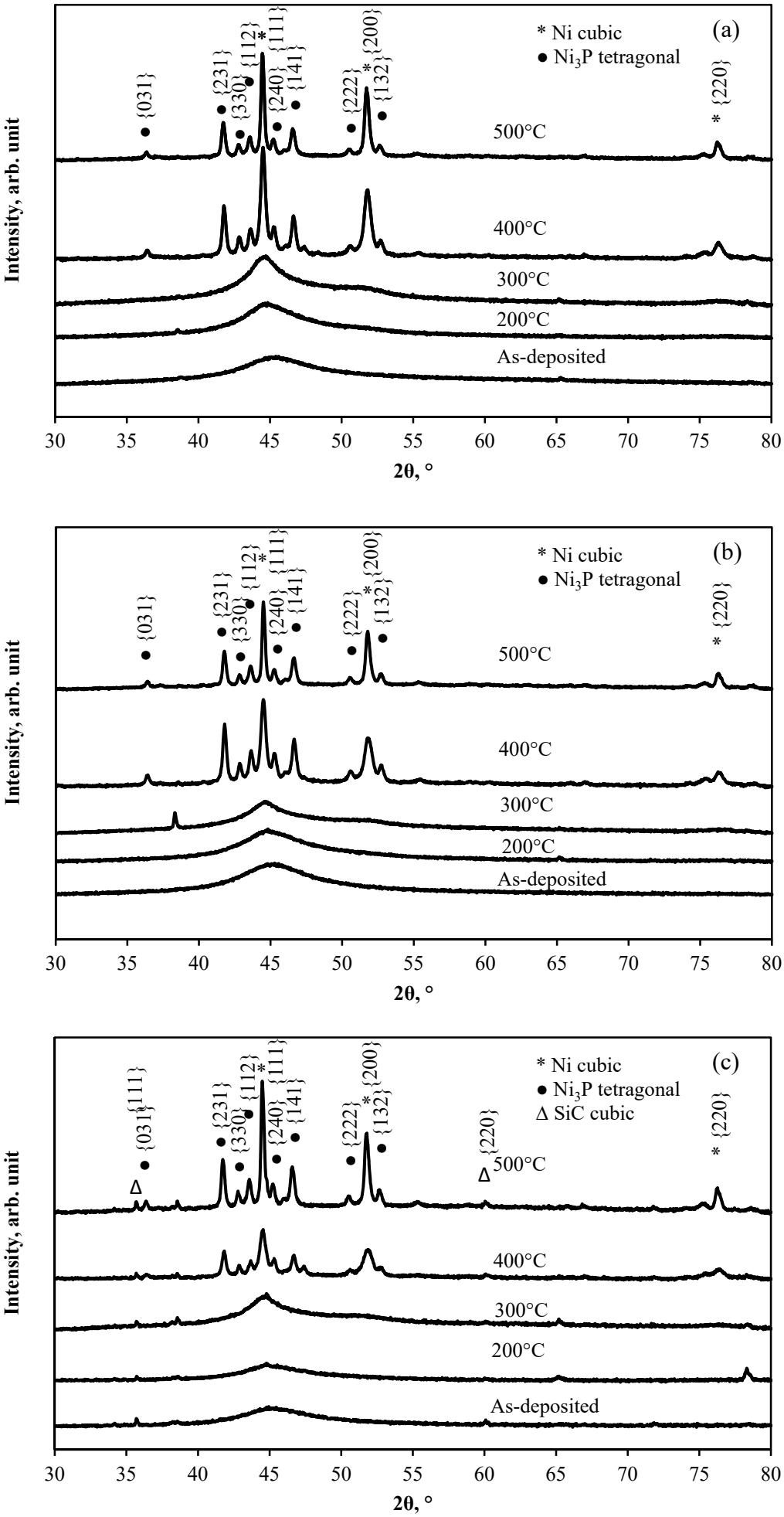
(a)
* Ni cubic
● Ni_3P tetragonal
{031}
{231}
{330}
{112}
{111}
{240}
{141}
{222}
{200}
{132}
{220}
500°C
400°C
300°C
200°C
As-deposited
Intensity, arb. unit
2θ, °
(b)
* Ni cubic
● Ni_3P tetragonal
500°C
400°C
300°C
200°C
As-deposited
Intensity, arb. unit
2θ, °
(c)
* Ni cubic
● Ni_3P tetragonal
Δ SiC cubic
{111}
500°C
400°C
300°C
200°C
As-deposited
Intensity, arb. unit
2θ, °

Fig. 1

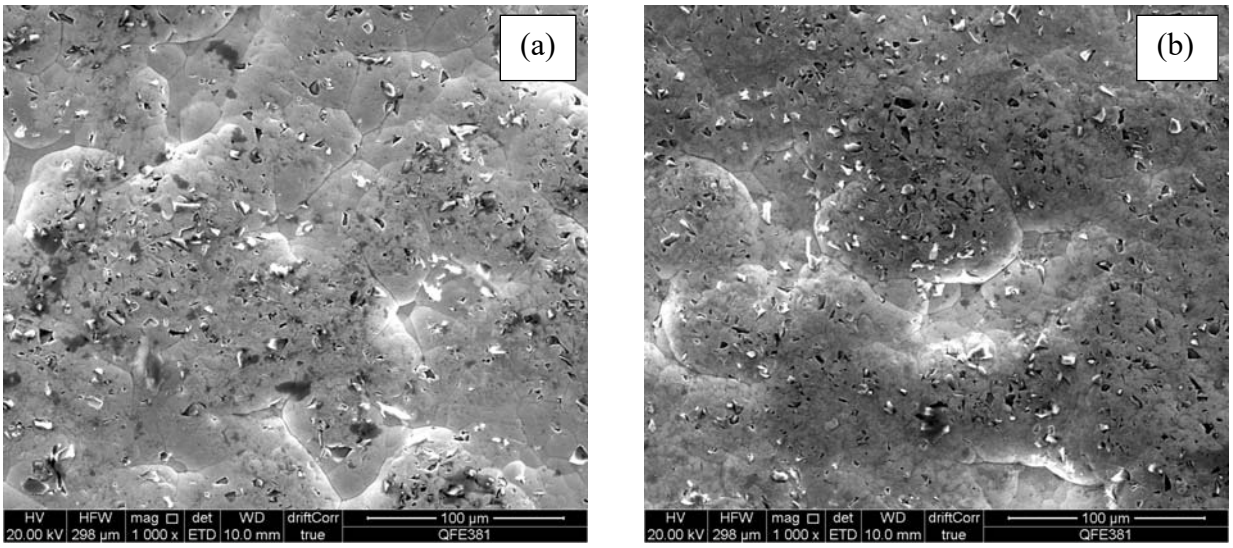
(a)
HV
20.00 kV
HFW
298 µm
mag
1 000 x
det
ETD
WD
10.0 mm
driftCorr
true
100 µm
QFE381
(b)
HV
20.00 kV
HFW
298 µm
mag
1 000 x
det
ETD
WD
10.0 mm
driftCorr
true
100 µm
QFE381

Fig. 2

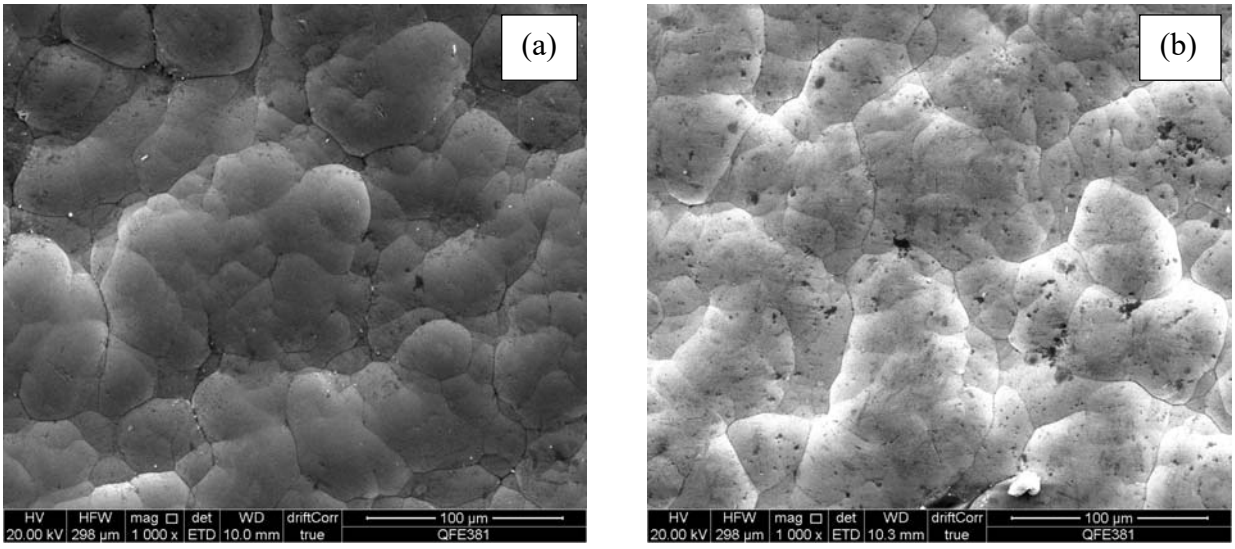
(a)
HV
20.00 kV
HFW
298 µm
mag
1 000 x
det
ETD
WD
10.0 mm
driftCorr
true
100 µm
QFE381
(b)
HV
20.00 kV
HFW
298 µm
mag
1 000 x
det
ETD
WD
10.3 mm
driftCorr
true
100 µm
QFE381

Fig. 3

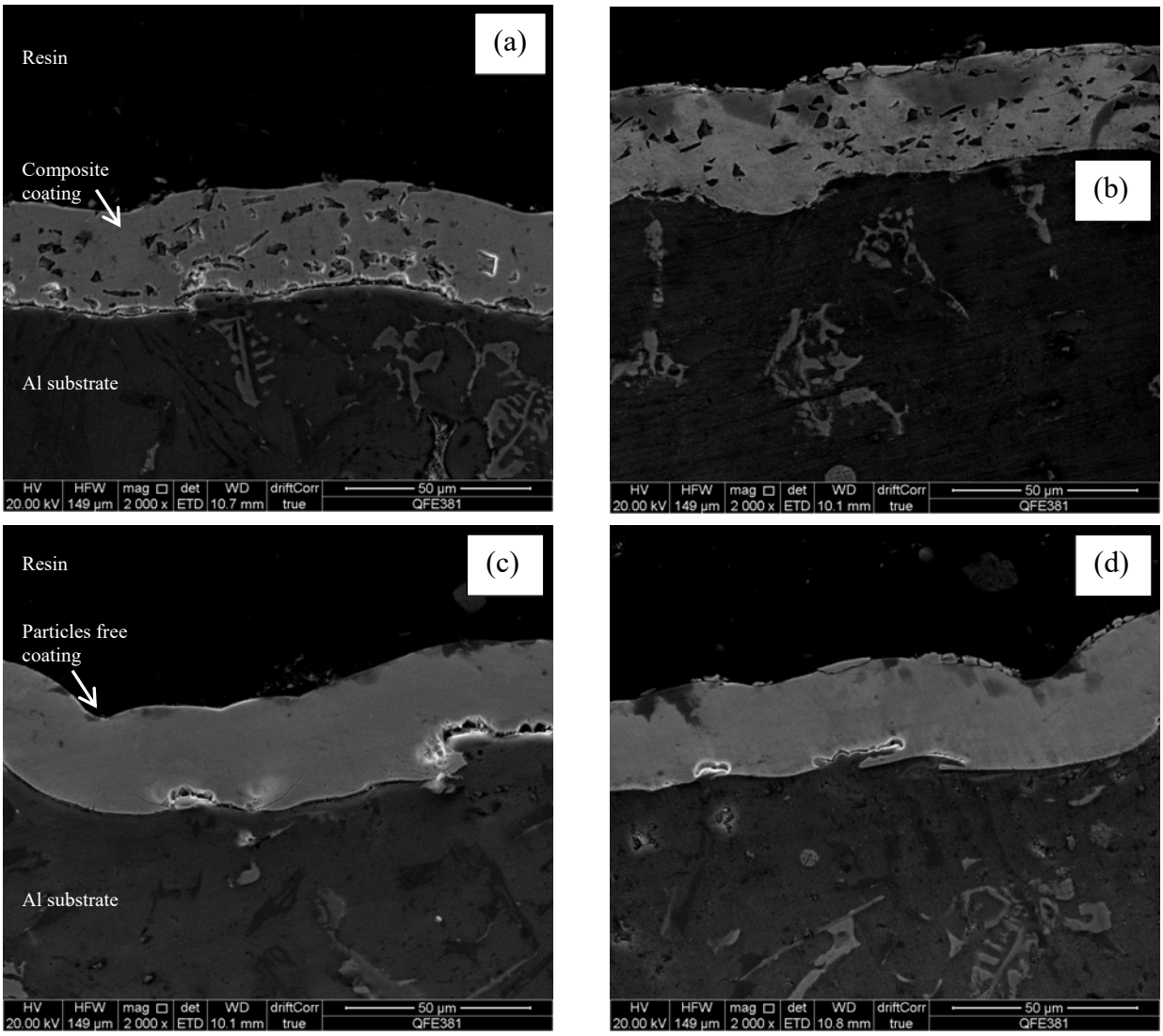
(a)
Resin
Composite coating
Al substrate
HV 20.00 kV
HFW 149 µm
mag 2 000 x
det ETD
WD 10.7 mm
driftCorr true
50 µm
QFE381
(b)
HV 20.00 kV
HFW 149 µm
mag 2 000 x
det ETD
WD 10.1 mm
driftCorr true
50 µm
QFE381
(c)
Resin
Particles free coating
Al substrate
HV 20.00 kV
HFW 149 µm
mag 2 000 x
det ETD
WD 10.1 mm
driftCorr true
50 µm
QFE381
(d)
HV 20.00 kV
HFW 149 µm
mag 2 000 x
det ETD
WD 10.8 mm
driftCorr true
50 µm
QFE381

Fig. 4

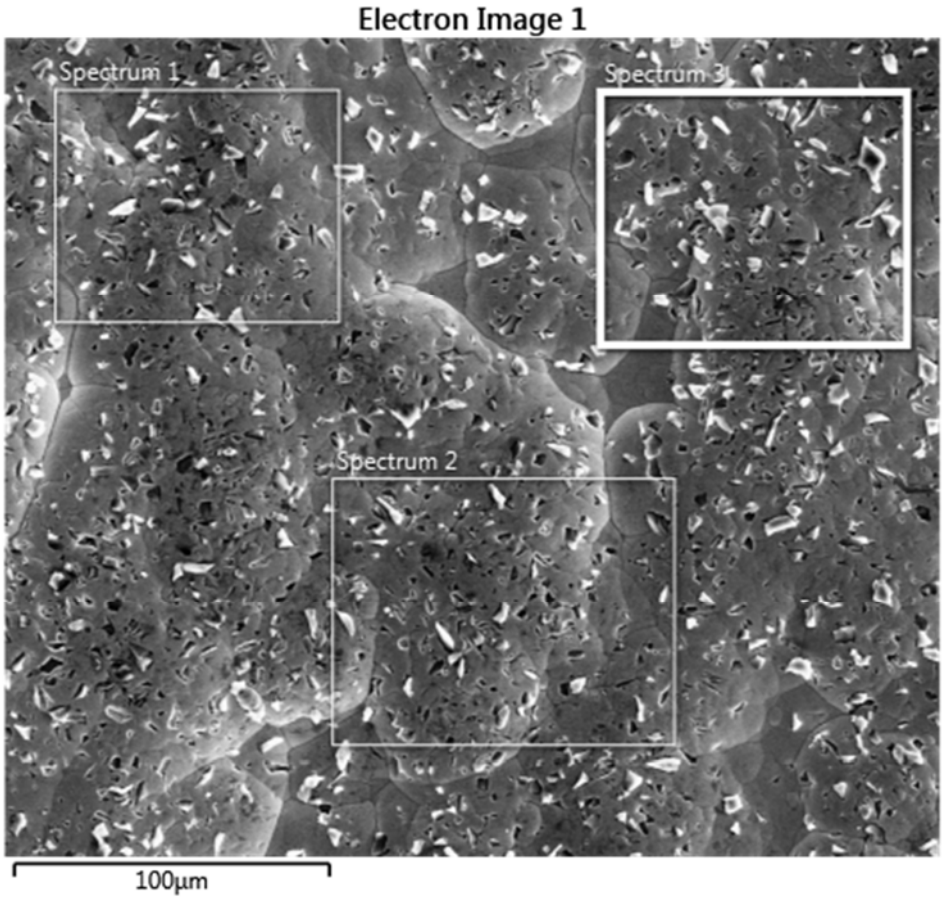

Fig. 5

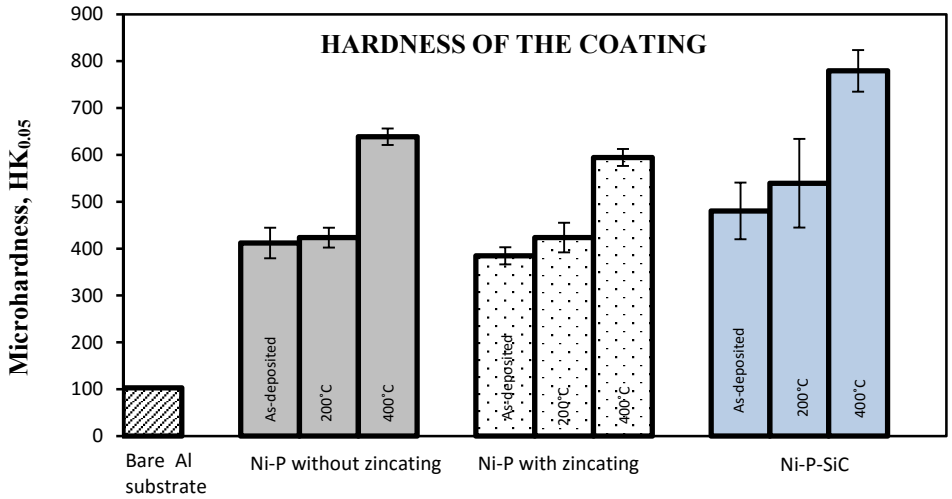
HARDNESS OF THE COATING
Microhardness, HK0.05
900
800
700
600
500
400
300
200
100
0
As-deposited
200°C
400°C
As-deposited
200°C
400°C
As-deposited
200°C
400°C
Bare Al substrate
Ni-P without zincating
Ni-P with zincating
Ni-P-SiC

Fig. 6

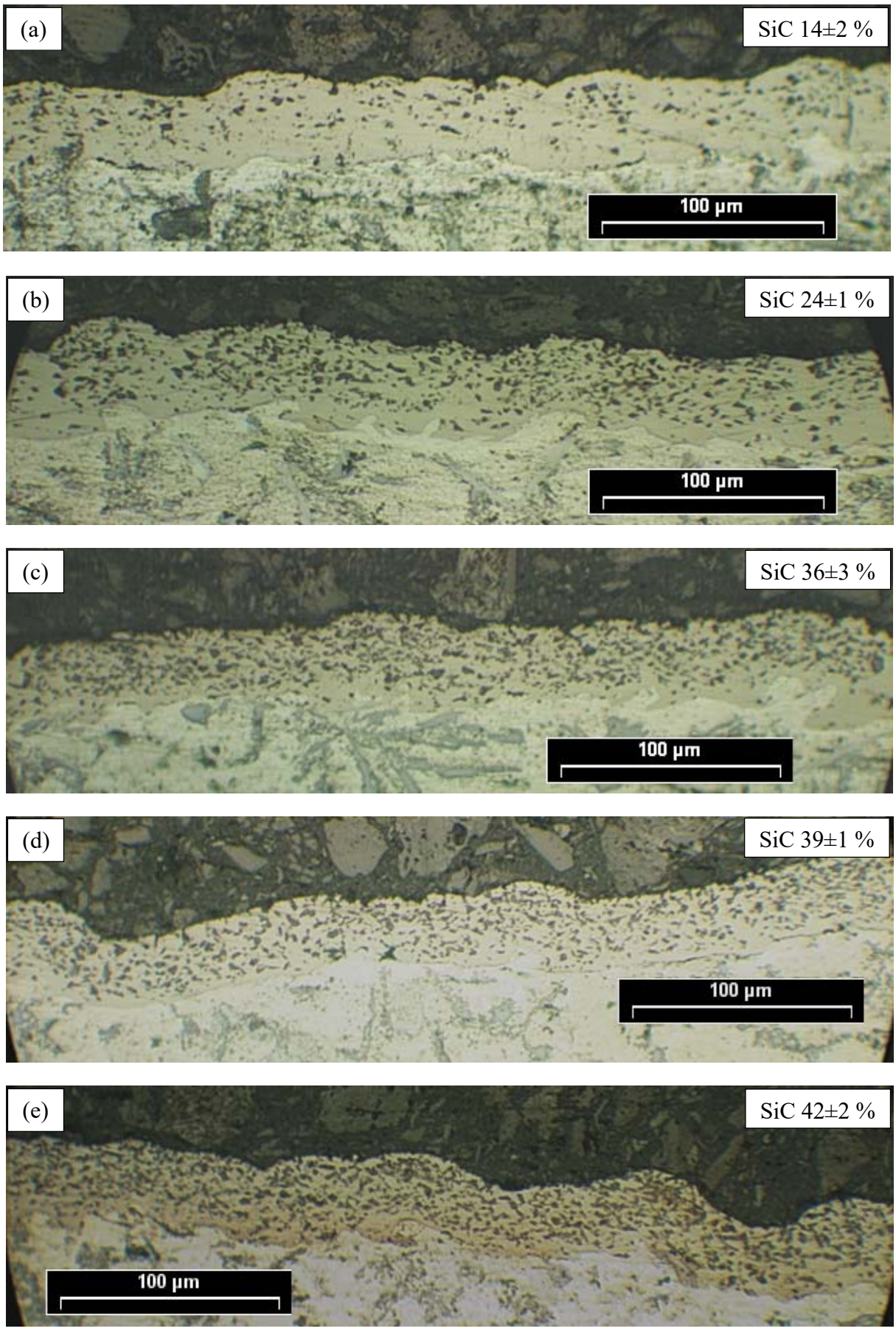
(a)
SiC 14±2 %
100 µm
(b)
SiC 24±1 %
100 µm
(c)
SiC 36±3 %
100 µm
(d)
SiC 39±1 %
100 µm
(e)
SiC 42±2 %
100 µm

Fig. 7

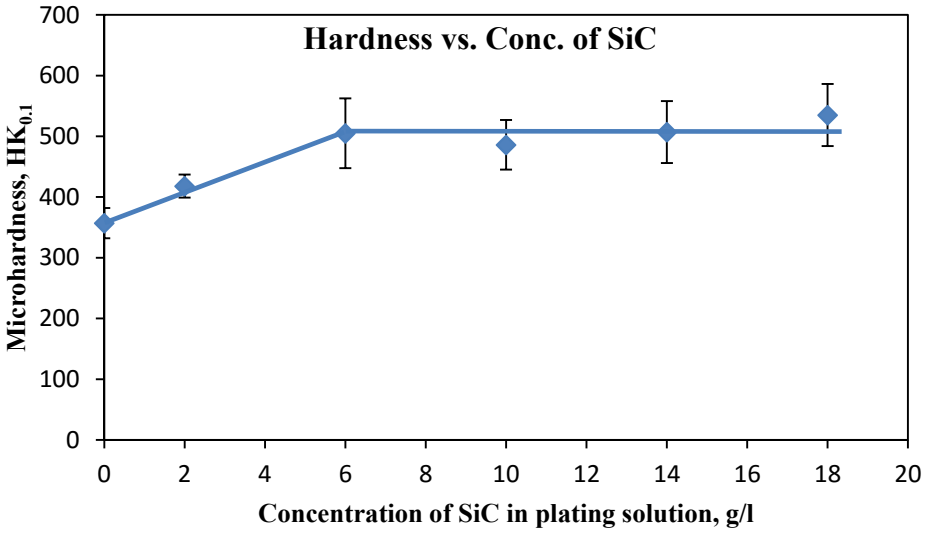
Hardness vs. Conc. of SiC
Microhardness, HK0.1
700
600
500
400
300
200
100
0
0
2
4
6
8
10
12
14
16
18
20
Concentration of SiC in plating solution, g/l

Fig. 8

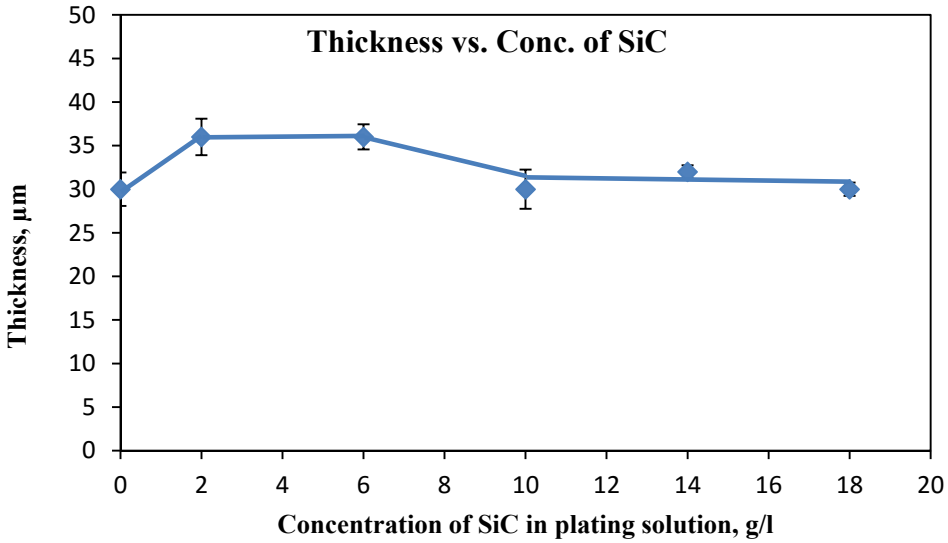
Thickness vs. Conc. of SiC
Thickness, µm
Concentration of SiC in plating solution, g/l
0
5
10
15
20
25
30
35
40
45
50
0
2
4
6
8
10
12
14
16
18
20

Fig. 9